

Improvement in Efficiency of Converter Transformer by The Reduction of Stray Losses

Jayesh U. Kothavade¹, Prasanta Kundu²

¹Electrical Engineering Department, S. V. National Institute of Technology, Surat, India (jayesh.kothavade@gmail.com),


²Electrical Engineering Department, S. V. National Institute of Technology, Surat, India (Pk@eed.svnit.ac.in)

Abstract

In High Voltage Direct Current Transmission (HVDC) system, converter transformer (CT) is an essential part of the system. Losses that occur in the CT are copper loss, stray loss, and core loss. The stray loss occurs in the transformer's metallic parts, such as transformer tank, which is 10% to 15% of the total loss. Current flowing through the CT is non-sinusoidal current, so more losses are produced in the CT than normal power transformer. In this paper, horizontal wall shunt is used to reduce stray loss in CT and compare the performance with vertical wall shunt. These stray losses calculated using the 3-D finite –element analysis (FEA). A 315 MVA CT is considered as a case study to calculate stray losses with and without wall shunt. Results show that the horizontal wall shunt is effective compared to vertical wall shunt; additionally, the stray loss is reduced as the wall shunt thickness is increased. Therefore, the efficiency of CT is increased due to a decrease in stray loss.

Keywords. Converter Transformer, horizontal wall shunt, vertical wall shunt, sinusoidal excitation, non-sinusoidal excitation, stray loss.

Type: Research Article

Open Access Peer Reviewed  CC BY

1. Introduction

Power consumption has been gradually growing in recent years, despite a minor rise in power generation. To meet the rising demand for electricity, a low-loss power transmission system is needed (Carrasco et al. 2006). For bulk power transmission, a high-voltage direct current transmission system (HVDC) is employed, which utilizes direct current (DC) for the transmission. HVDC allows power transmission between grids with different frequencies (such as 50 Hz and 60 Hz) and unsynchronized AC transmission systems (Alassi et al. 2019). The generating station, converter transformer, converters, dc line, and inverter station are the key components of an HVDC system.

A converter transformer (CT) is an important component of a high-voltage direct current (HVDC) system. It serves as a connection between the connected alternating current (AC) grids and the high-power rectifiers. It generates a phase shift and insulates the rectifier from the AC grid. Generally, the efficiency of the transformer is nearer to 90% (Li et al. 2014). So, if there is a slight increase in efficiency by reducing transformer loss, it could be a more power economic-benefit. Stray losses occur in the transformer's metal parts due to leakage field produced by the winding in nearer metal parts i.e. tank (Moghaddami, Sarwat, and De Leon 2016, Del Vecchio et al. 2017, Basak and Kendall 1987, Kuczmann, Szücs, and Kovács, Hajiaghasi, Abbaszadeh, and Salemnia 2019, Thango and Bokoro 2022). These stray losses

are nearly 10% to 15% of the total losses, which causes local hot-spot of temperature rise in transformer (Li et al. 2015, Janić, Valković, and Štih 2006, Orosz et al. 2015, Jamali, Mirzaie, and Gholamian 2011). CT's secondary and tertiary winding is connected to the bridge rectifier and due to the sequence operation of switches in bridge rectifier, the current flow through the CT's winding is non-sinusoidal (Kulkarni and Khaparde 2004, Kothavade and Kundu 2021); therefore, the losses are larger than in a normal transformer (Orosz, Borbély, and Tamus 2017, Miguéis, Guimarães, and Borges 2017). So, magnetic wall shunts are used to minimize stray losses in CT. The leakage fluxes are prevented from reaching the transformer tank by these magnetic wall shunts, which provides a low reluctance path. The material used for magnetic wall shunt is laminated electrical steel.

Practically, it is difficult to estimate the transformer's stray losses and the magnetic wall shunt's optimum location (Thango, Jordaan, and Nnachi 2021). Therefore, in ANSYS MAXWELL-3D simulation, the 3-D finite-element analysis (FEA) approach is employed.

The detailed description steps for designing the core, winding, and tank are studied in (Sawhney and Chakrabarti 2006, Dasgupta 2009). In (Kimbark 1971) discuss the operation of a three-phase and a single-phase rectifier, the HVDC system's purpose and its limitations are presented. Analysis of bridge converter with different overlap angle is also discussed. While (Carlson 1996) showed the various CT functions and stress distribution due to DC voltage and AC voltage applied on the transformer winding. (Kulkarni and Khaparde 2004, Committee 2003, Wang et al. 2003) provides detailed information on insulation design, rating, various configuration of CT. Magnetic wall shunts different structures, and optimum placing in power transformer using FEA is explained in (Hernandez, Arjona, and Sturgess 2006, Song et al. 2011). Vertical wall shunt and the effect of change in thickness of wall shunt in a power transformer are addressed in (Committee 2003, Park, Lee, and Hahn 2019). Horizontal and vertical shunt comparisons and magnetic wall shunt impact are studied in (Moghaddami, Sarwat, and De Leon 2016, Djurovic and Monson 1982, Djurovic and Monson 1977, Susnjic, Haznadar, and Valkovic 2008).

In this paper, for reducing stray losses, a horizontal wall shunt arrangement is used; also, its effectiveness compares with the vertical wall shunt arrangement in CT. This paper's novelty is that both types of wall shunt arrangements are proposed for non-sinusoidal current excitation and the fundamental component of the non-sinusoidal current excitation for three winding CT. The effect of change in the thickness of wall shunt for both arrangements is investigated in this paper. All these results are analysed using the 3-D FEA method in ANSYS-MAXWELL. Also, stray losses are calculated using the analytical method and compared with the 3-D FEA method.

2. Theory

2.1. Converter Transformer Bridge Connection

In CT, primary winding is connected to the AC supply, and secondary windings legs are connected to the bridge rectifier, as shown in **Figure 1**. In this **Figure 1** one 2 winding transformer is utilized for six pulse operation but for twelve pulse operation, two 2 winding transformer (star-delta and star-star type) or one 3 winding transformer can be utilized (Kulkarni and Khaparde 2004). The diodes sequence of operation and a current running through the winding is shown in **Figure 2** Each diode will conduct for 120° .

By Fourier analysis, the crest value of the fundamental component of the waveform shown in **Figure 2** is given by **Equation (2)** (Kulkarni and Khaparde 2004, Kimbark 1971).

$$\sqrt{2} I_{L1} = \frac{2}{\pi} \int_{-\pi/3}^{\pi/3} I_d \cos \theta d\theta = \frac{2}{\pi} I_d [\sin \theta]_{-\pi/3}^{\pi/3} = \frac{2\sqrt{3}}{\pi} I_d = 1.11 I_d \tag{1}$$

RMS value of fundamental current is,

$$I_{L1} = \frac{\sqrt{6}}{\pi} I_d = 0.78 I_d \tag{2}$$

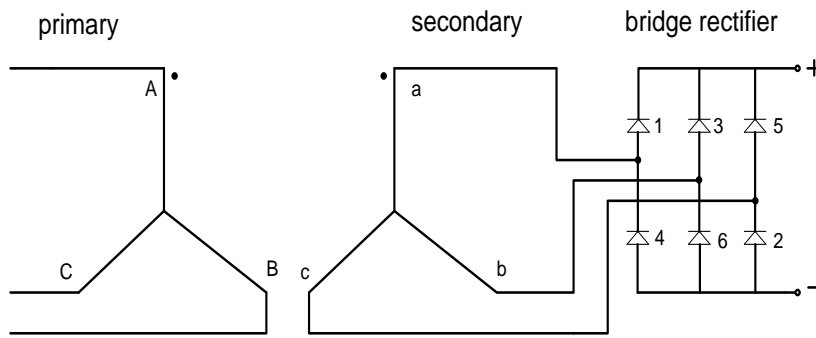


Figure 1: Bridge Connection

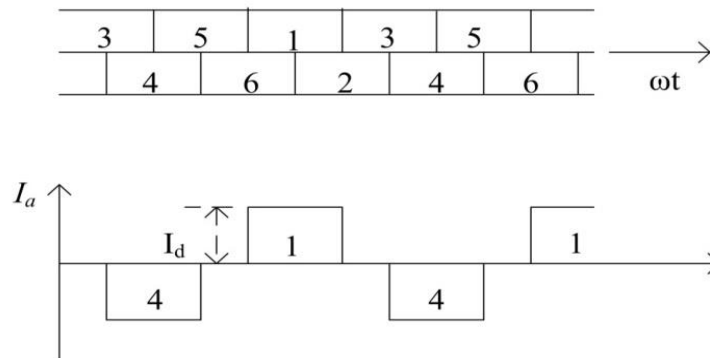


Figure 2: Sequence Operation of Diode and Secondary Winding Current

2.2. Power factor Calculation for Non-Sinusoidal Waveform

The non-sinusoidal waveform can be mathematically split up into its individual components called the fundamental frequency and a number of harmonic frequencies for power factor (pf) calculation, using the Fast Fourier Transform (FFT). Steps for pf calculation of non-sinusoidal waveform is shown below (Langella and Testa 2010, Poblador and López 2013).
 Active Power=

$$P = \{|V_1| * |I_1| \cos \phi_1 + |V_H| * |I_H| \cos \phi_H\} / 2 \tag{3}$$

Since,

$$\vec{V}_1 = |V_1| \angle \theta_1, \vec{I}_1 = |I_1| \angle \theta_1$$

$$\vec{V}_H = |V_H| \angle \theta_H ; \quad \vec{I}_H = |I_H| \angle \theta_H$$

Where,

\vec{V}_1 = Fundamental harmonic component of the maximum voltage;

\vec{I}_1 = Fundamental harmonic component of the maximum current;

\vec{V}_H = All integer number of harmonic component of the maximum voltage except h=1;

\vec{I}_H = All integer number of harmonic component of the maximum current except h=1;

ϕ_1 = Angle between \vec{V}_1 and \vec{I}_1

ϕ_H = Angle between \vec{V}_H and \vec{I}_H

The values of \vec{V}_1 , \vec{I}_1 , \vec{V}_H and \vec{I}_H are obtained from FFT report.

Reactive Power =

$$Q = \{|V_1| * |I_1| \sin \phi_1 + |V_H| * |I_H| \sin \phi_H\} / 2 \quad (4)$$

$$\phi = \tan^{-1} \left(\frac{Q}{P} \right) \quad (5)$$

$$\therefore pf = \cos \phi \quad (6)$$

2.3 Stray Loss

Eddy current induces power loss in the transformer tank, and this eddy current is caused by leakage flux in the winding. The power loss in the transformer tank is known as stray loss, and it can be calculated using the Poynting vector. The stray loss is calculated using Maxwell's equations (Kulkarni and Khaparde 2004, Park, Lee, and Hahn 2019, Matthew 2015).

$$\nabla \times E = - \frac{\partial B}{\partial t} \quad (7)$$

$$\nabla \times H = J \quad (8)$$

$$\nabla \cdot B = 0 \quad (9)$$

There are two constitutive relations.

$$B = \mu H \quad (10)$$

$$J = \sigma E \quad (11)$$

Where

H = magnetic field strength (A/m),
 E = electric field strength (V/m),
 B = flux density (Wb/m²), J = current density (A/m²),
 μ = permeability of material (henrys/m),
 σ = conductivity (mhos/m).

Taking curl on both sides of equation (8) and simplify using vector algebra.

$$\nabla(\nabla \cdot H) - \nabla^2 H = \nabla \times J \tag{12}$$

Using equations (7), (9), (10) and (11), the equation(12) is expressed as.

$$\nabla^2 H - \mu\sigma \frac{\partial H}{\partial t} = 0 \tag{13}$$

Assume a structural component, as presented in **Figure 3**. The magnetic field intensity H_y and current density J_x are considered to be the functions of z . The complex permeability can be written as Equation (13) for this problem.

$$\frac{d^2 H_y}{dz^2} = j\omega\sigma\mu H_y \tag{14}$$

At $z=0$, $H_y = H_a$ At $z=\infty$, $H_y = 0$

By simplifying equation (14) from above condition,

$$H_y = H_a e^{-mz} \tag{15}$$

$$m = \sqrt{j\omega\sigma\mu} = (1 + j)\sqrt{\frac{\omega\sigma\mu}{2}} \tag{16}$$

Where H_a is a constant and m is propagation constant.

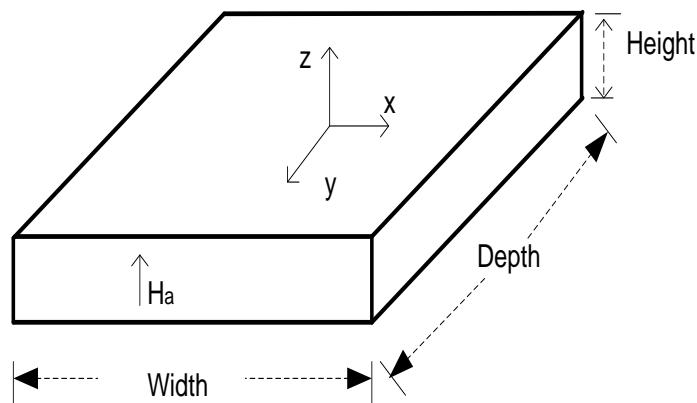


Figure 3: Stray Loss in Structural Components

By solving equation (15) and (16),

$$H_y = H_a e^{-\frac{(1+j)z}{\delta}} \tag{17}$$

Substituting equation (17) in equation (8) and simplify using vector algebra.

$$J_x = \frac{(1+j)}{\delta} H_a e^{-\frac{(1+j)z}{\delta}} \tag{18}$$

Calculating the real part of the complex Poynting vector at the surface gives the time-averaged density of the stray loss from the transformer tank.

$$P = \frac{1}{2} \text{Re}[E \times H^*] \tag{19}$$

On the surface ($z = 0$), substitute equation (17) and (18) in equation (19).
 The stray loss per unit surface area is,

$$P = \frac{1}{2} \text{Re}[E \times H^*]$$

$$\therefore P = \frac{1}{2} \frac{H_a^2}{\sigma \delta}$$

$$P = \sqrt{\frac{\mu \omega}{2\sigma}} \frac{H_a^2}{2} \tag{20}$$

Therefore, the transformer tank's total power loss is,

$$P = \sqrt{\frac{\mu \omega}{8\sigma}} \int_{\text{surface}} H_a^2 ds \tag{21}$$

3. System Development

In this paper, Rihand HVDC station (Rihand-Delhi HVDC scheme) CT specification is considered for designing a transformer(Committee 2003). The specification of the transformer is given in **Table 1**.

Classification	Value
MVA rating	315 MVA, 1 \emptyset , 3 winding
Line Winding Voltage (HV)	$\frac{400}{\sqrt{3}}$ kV
Valve Winding Voltage (LV)	$\frac{213}{\sqrt{3}}$ kV star and 213 kV delta

Table 1: Specification Of CT

Figure 4 shows that the designed CT in ANSYS-MAXWELL-3D 19.0 software. For the reduction of stray losses in CT, horizontal wall shunt and vertical wall shunt is used. **Figure 5(a)** and **(b)** shows the 315MVA CT with vertical wall shunt and horizontal wall shunt respectively. Vertical wall shunt is parallel to the high voltage (HV) winding, shown in **Figure 5(a)**. Horizontal wall shunt is parallel to the yoke, which is shown in **Figure 5(b)**. Dimensions of the transformer tank and wall shunt are given in **Table 2**.

Quantity	Dimensions in mm
Transformer Tank	5905 × 2198 × 8120
Vertical plates of wall shunt	380 × x × 4820
Horizontal plates of wall shunt	5600 × x × 380

Table 2: Dimensions of the transformer tank and wall shunt

Where x is the thickness of the wall shunt. For this paper, two cases of wall shunt thickness are considered, i.e. 10mm and 20mm.

In vertical wall shunt, the transformer's front and backside are provided with 10 vertical plates of wall shunt each, whereas left and right side of the transformer is provided with 5 vertical wall shunt each as shown in **Figure 5(a)**. There is 30 total number of vertical wall shunt used in **Figure 5(a)**. The dimensions of the vertical plates of the wall shunt are given in **Table 2**.

In horizontal wall shunt, the transformer's front and backside are provided with 6 horizontal plates of wall shunt each; whereas the left and right side of the transformer is provided with 4 vertical wall shunt each as shown in **Figure 5(b)**. There are 12 horizontal plates and 8 vertical plates of wall shunt used in **Figure 5(b)**. Dimensions of the vertical and horizontal plates of the wall shunt are given in **Table 2**.

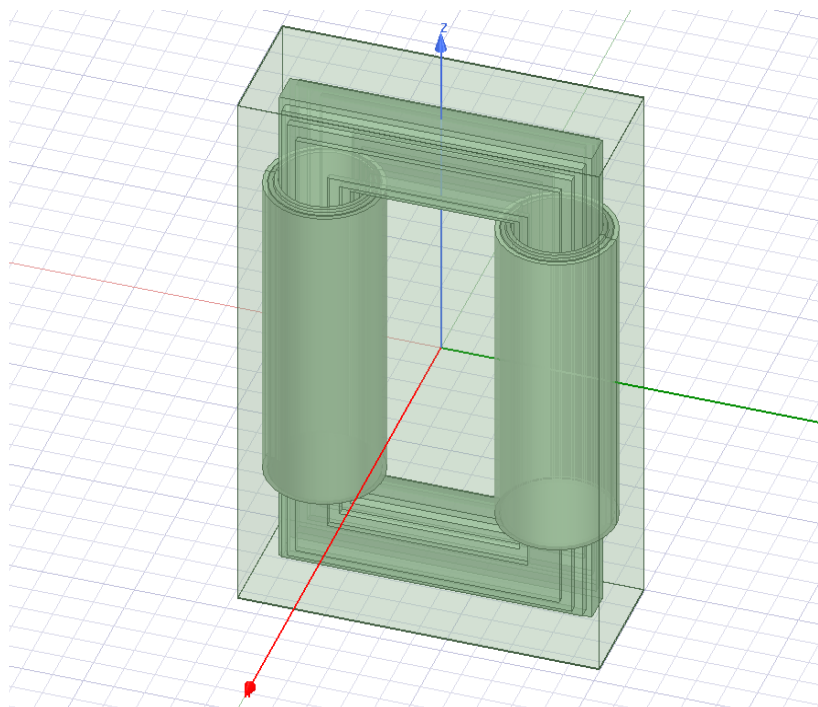


Figure 4: 315 MVA Converter Transformer without Wall Shunt

The materials used for core, winding, tank, and wall shunt are JFE_Steel_35, copper, steel_1008, and M5 respectively. For the CT, the nature of the current waveform is non-

sinusoidal, shown in **Figure 2**. For the CT's simulation, two major cases of current excitation are considered a) Sinusoidal excitation b) Non-sinusoidal excitation. For sinusoidal excitation, CT is excited with the rated current value, which is a fundamental component of non-sinusoidal excitation. In non-sinusoidal excitation, CT is excited with non-sinusoidal excitation whose value obtained from **equation (2)**. For the reduction of stray losses, transformer tank is provided with a magnetic wall shunt. The effect of change in thickness of wall shunt on the stray loss is analysed with two cases, i.e. 10 mm and 20 mm.

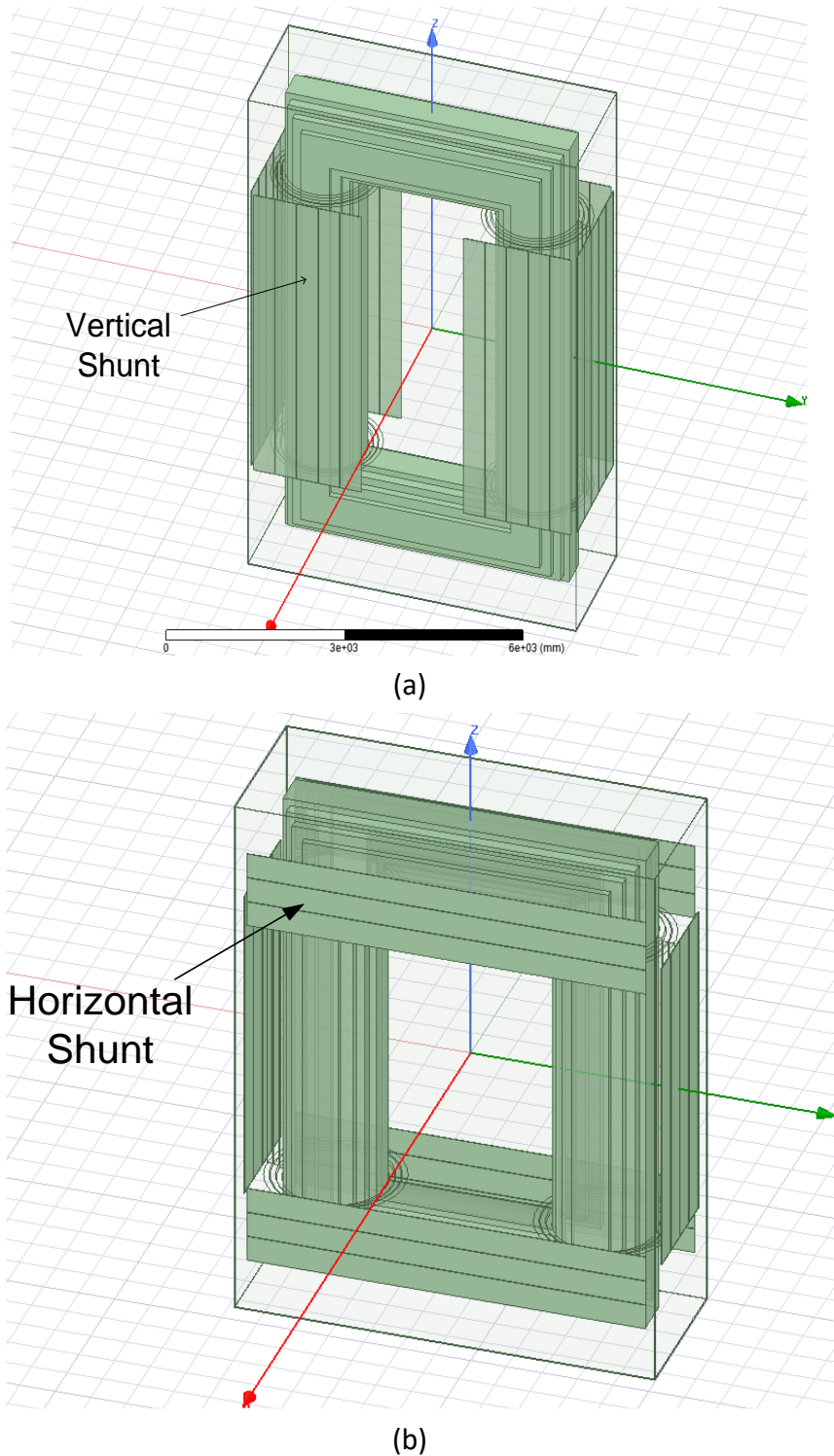


Figure 5: 315 MVA Single Phase Three Winding Converter Transformer a) Vertical Wall Shunt b) Horizontal Wall Shunt

4. Simulation Results and Discussion

In this section, 315 MVA CT’s efficiency is calculated on full load in which loading given to the transformer is resistive load.

4.1. Vertical Shunt

In this section, vertical wall shunt is used for the reduction of stray losses in CT. This vertical wall shunt is parallel to HV winding shown in **Figure 5(a)**.

4.1.1. Sinusoidal Current Excitation

In this case, CT’s low voltage (LV) winding is excited by sinusoidal current excitation in which rms value of the rated current is 2.561 kA. For the efficiency calculation at full load, CT’s secondary winding i.e. medium-voltage (MV) and tertiary winding i.e. HV is loaded by 144.11 Ω and 169.43 Ω respectively.

4.1.1.1 CT with Tank

In this case, the designed CT shown in **Figure 4** is simulated in ANSYS-MAXWELL 19.0 software. **Figure 6**, **Figure 7** and **Figure 8** show induced voltage and current waveform of LV, MV and HV winding respectively. The average value of stray loss is 114.15 kW which is obtained from **Figure 9**.

Efficiency is calculated using **equation (22)**,

$$\% \eta = \frac{\text{output}}{\text{input}} = \frac{V_b I_b \cos \theta_b + V_c I_c \cos \theta_c}{V_a I_a \cos \theta_a} \times 100 \tag{22}$$

Where

- V_a = Voltage in LV winding,
- I_a = Current in LV winding,
- θ_a = Angle between V_a and I_a ,
- V_b = Voltage in MV winding,
- I_b = Current in MV winding,
- θ_b = Angle between V_b and I_b ,
- V_c = Voltage in HV winding,
- I_c = Current in HV winding,
- θ_c = Angle between V_c and I_c

The pf of the LV winding obtained from **Figure 6** is 0.83 and efficiency is 90.38%.

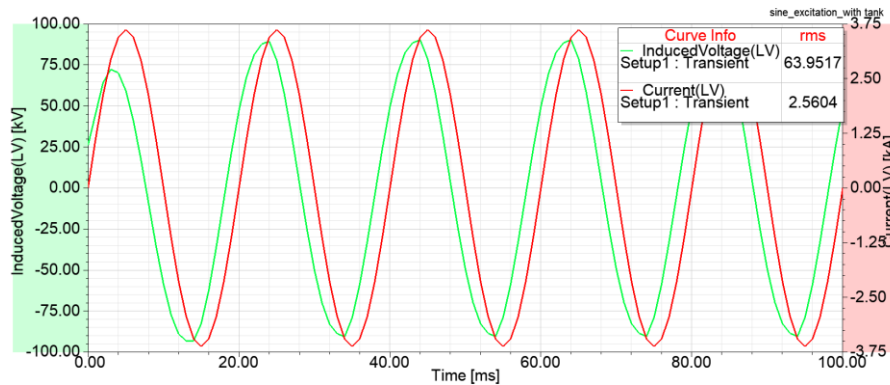


Figure 6: Waveform of LV Winding Induced Voltage and Current

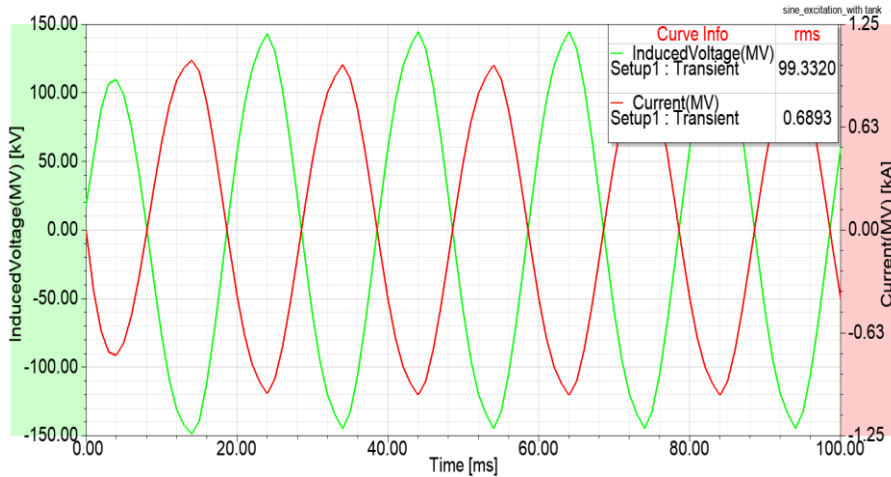


Figure 7: Waveform of MV Winding Induced Voltage and Current

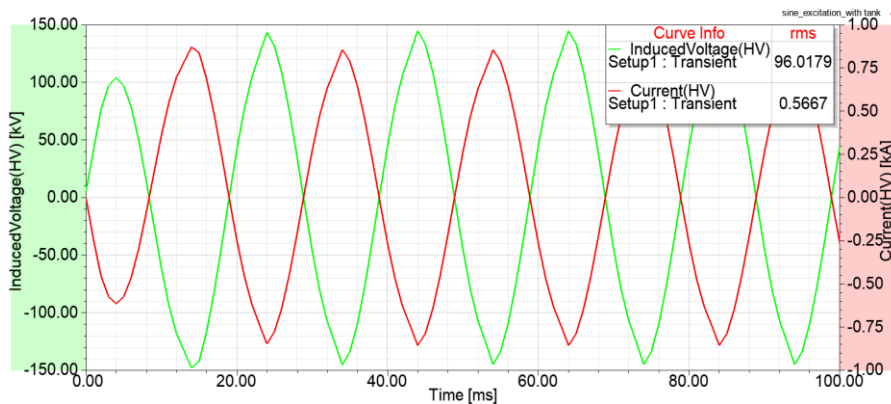


Figure 8: Waveform of HV Winding Induced Voltage and Current

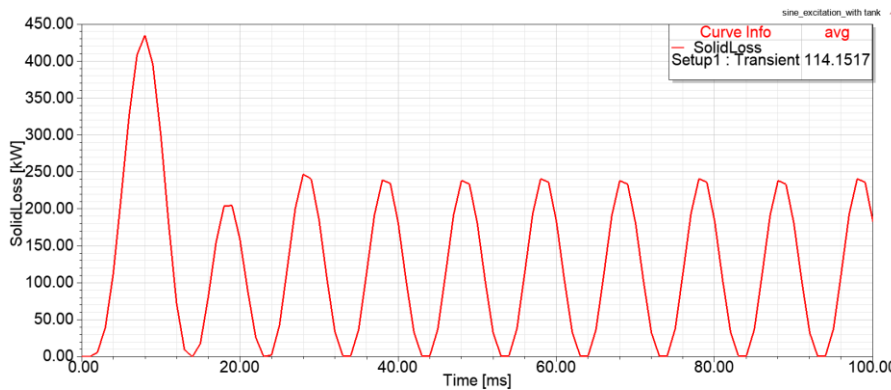


Figure 9: Waveform of Stray Loss

4.1.1.2 CT with 10 mm wall shunt

In this case, the designed CT with 10 mm wall shunt thickness shown in **Figure 5(a)** is simulated. **Figure 10** and **Figure 11** shows induced voltage and current waveform of LV, MV and HV winding. The average value of the stray loss is 43.90 kW which is obtained from **Figure 12**.

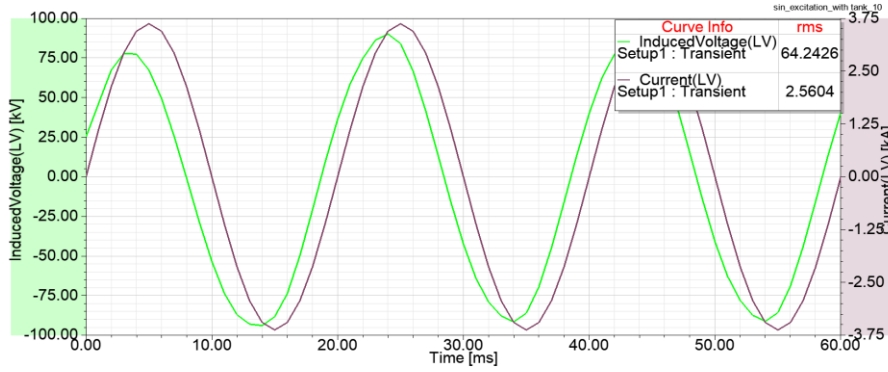


Figure 10: Waveform of LV Winding Induced Voltage and Current

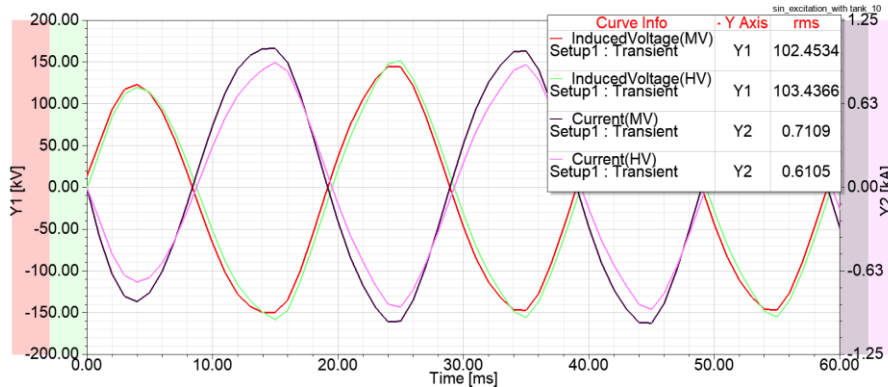


Figure 11: Induced Voltage and Current Waveforms of MV and HV Winding

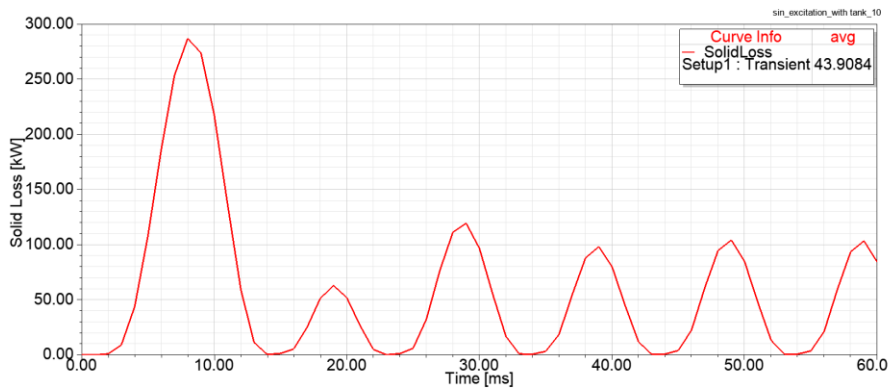


Figure 12: Waveform of Stray Loss

The pf of the LV winding obtained from Figure 10 is 0.88 and efficiency is 93.85%.

4.1.1.3 CT with 20 mm wall shunt

In this case, the designed CT with 20 mm wall shunt thickness is simulated. Figure 13 and Figure 14 shows induced voltage and current waveform of LV, MV and HV winding. The average value of the stray loss is 18.90 kW which is obtained from Figure 15.

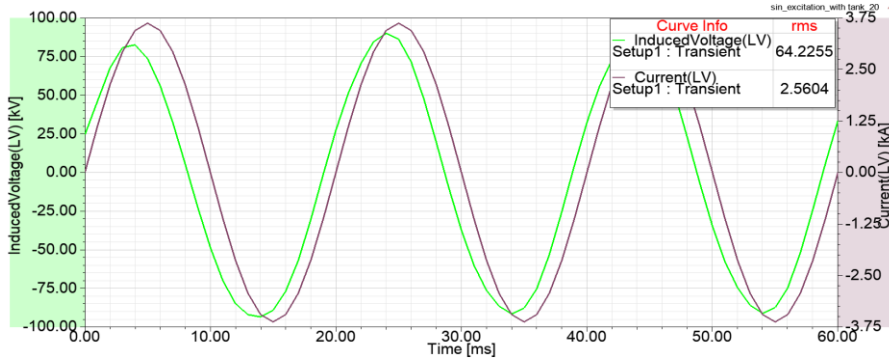


Figure 13: Waveform of LV Winding Induced Voltage and Current

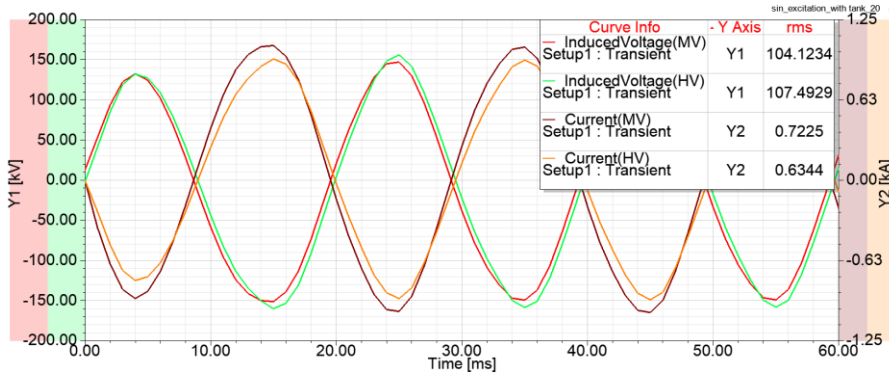


Figure 14: Induced Voltage and Current Waveforms of MV and HV Winding

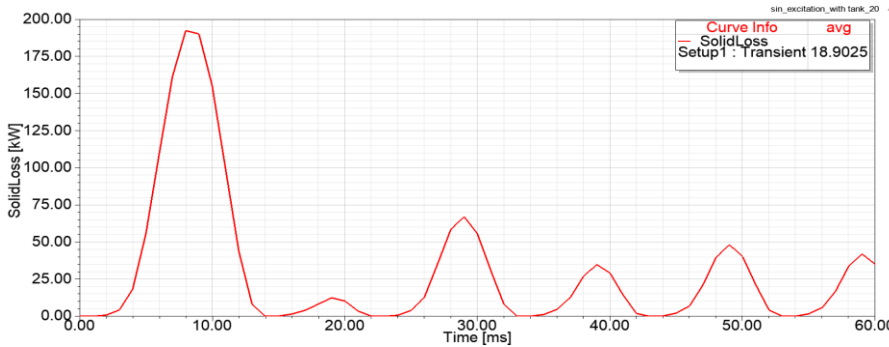


Figure 15: Waveform of Stray Loss

The pf of the LV winding obtained from **Figure 13** is 0.91 and efficiency is 95.51%.

4.1.2. Non-Sinusoidal Current Excitation

In this case, CT's design remains the same as the sinusoidal excitation case; the only change is the non-sinusoidal excitation given in this case. The nature of the non-sinusoidal current excitation waveform is shown in **Figure 2** LV winding is excited with a peak value of the current is 3.283 kA. For the efficiency calculation at full load, CT's secondary winding i.e. MV and tertiary winding i.e. HV is loaded by 88.17 Ω and 104.04 Ω respectively.

4.1.2.1 CT with Tank

After simulation, induced voltage and current waveform of LV, MV and HV winding is shown in **Figure 16** and **Figure 17**. The average value of the stray loss is 215.4 kW which is obtained from **Figure 18**.

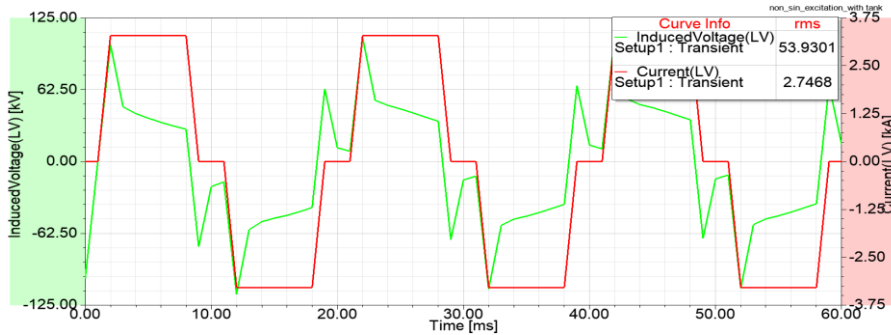


Figure 16: Waveform of LV Winding Induced Voltage and Current

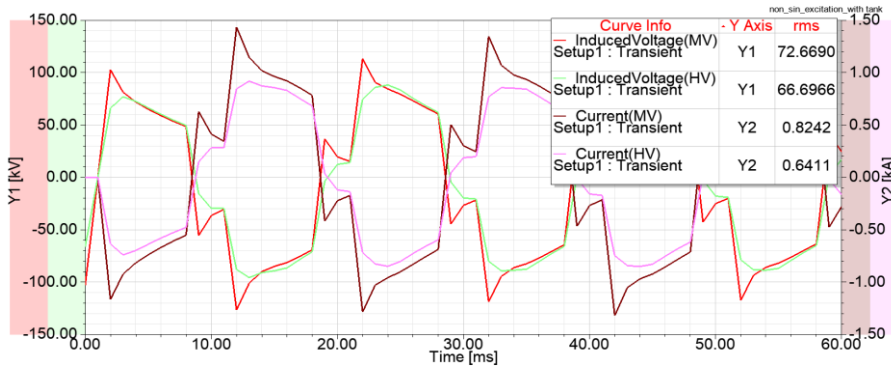


Figure 17: Induced Voltage and Current Waveforms of MV and HV Winding

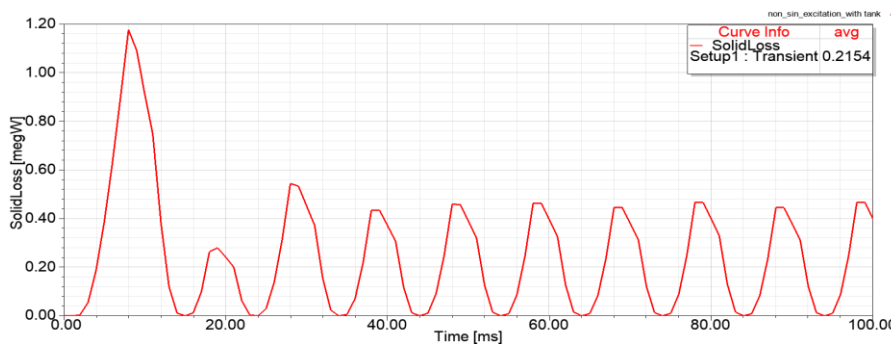


Figure 18: Waveform of Stray Loss

Using FFT analysis, the pf of the LV winding is found to be 0.88, and efficiency is 78.91%.

4.1.2.2 CT with 10 mm wall shunt

After simulation, induced voltage and current waveform of LV, MV and HV winding is shown in Figure 19 and Figure 20. The average value of the stray loss is 63.52 kW which is obtained from Figure 21.

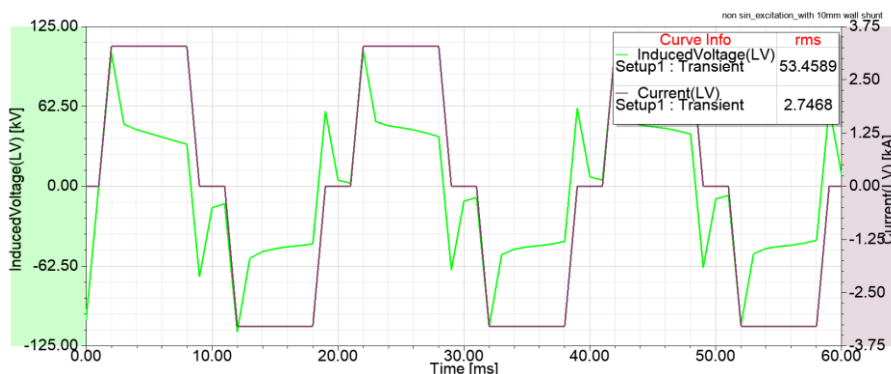


Figure 19: Waveform of LV Winding Induced Voltage and Current

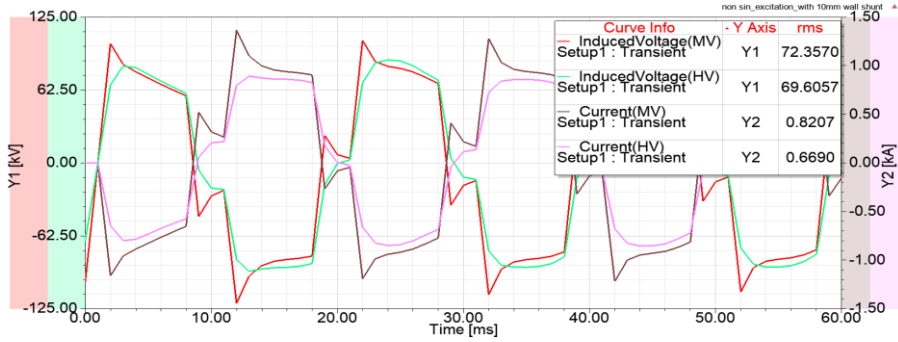


Figure 20: Induced Voltage and Current Waveforms of MV and HV Winding

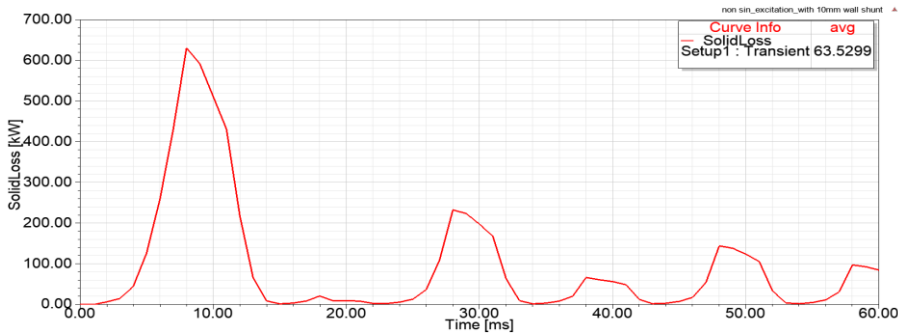


Figure 21: Waveform of Stray Loss

4.1.2.3 CT with 20 mm wall shunt

After simulation, induced voltage and current waveform of LV, MV and HV winding is shown in Figure 22 and Figure 23. The average value of the stray loss is 33.74 kW which is obtained from Figure 24.

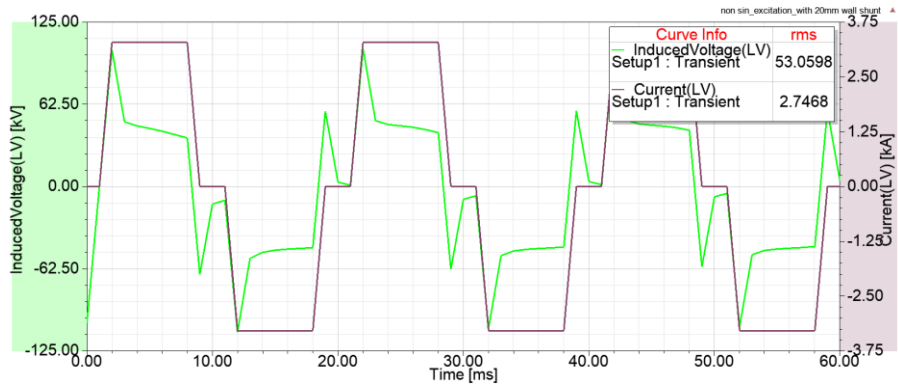


Figure 22: Waveform of LV Winding Induced Voltage and Current

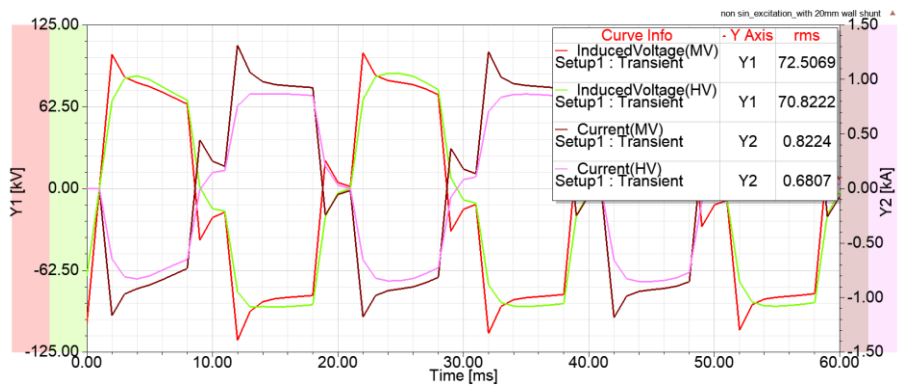


Figure 23: Induced Voltage and Current Waveforms of MV and HV Winding

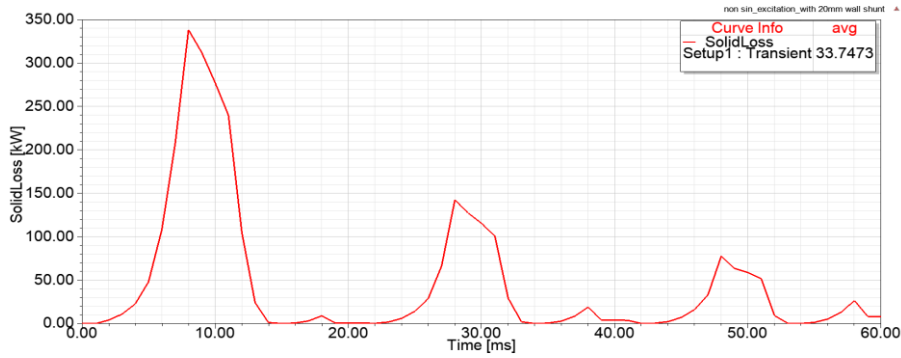


Figure 24: Waveform of Stray Loss

Using FFT analysis, the pf of the LV winding is found to be 0.92, and efficiency is 80.39%.

4.2. Horizontal Shunt

In this section, the reduction of stray losses in CT horizontal wall shunt is used in place of vertical wall shunt. This horizontal wall shunt is in parallel to the yoke shown in **Figure 5(b)**.

4.2.1. Sinusoidal Current Excitation

In this section, current excitation and loading values are the same as the previous sinusoidal excitation case with a vertical shunt.

4.2.1.1 CT with 10 mm wall shunt

After simulation, induced voltage and current waveform of LV, MV and HV winding is shown in **Figure 25** and **Figure 26**. The average value of the stray loss is 42.29 kW which is obtained from **Figure 27**.

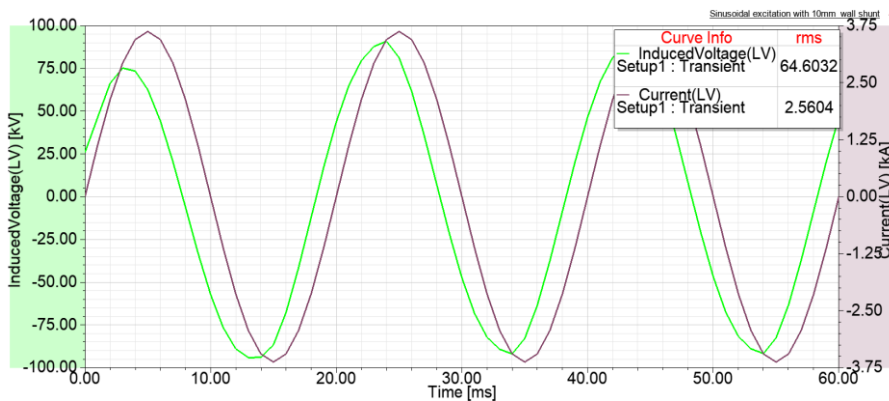


Figure 25: Waveform of LV Winding Induced Voltage and Current

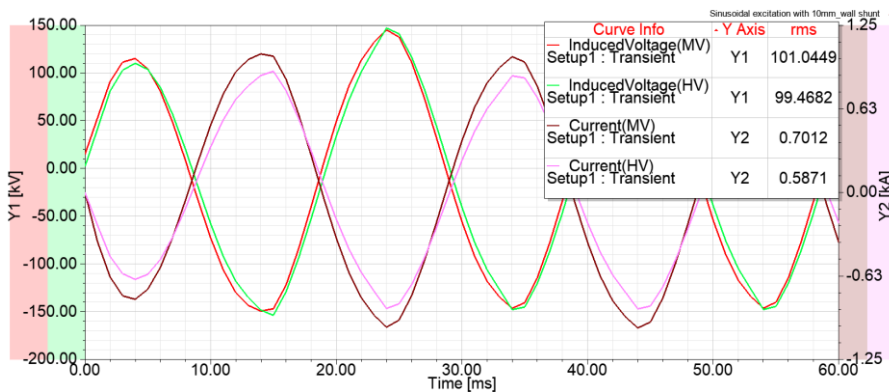


Figure 26: Induced Voltage and Current Waveforms of MV and HV Winding

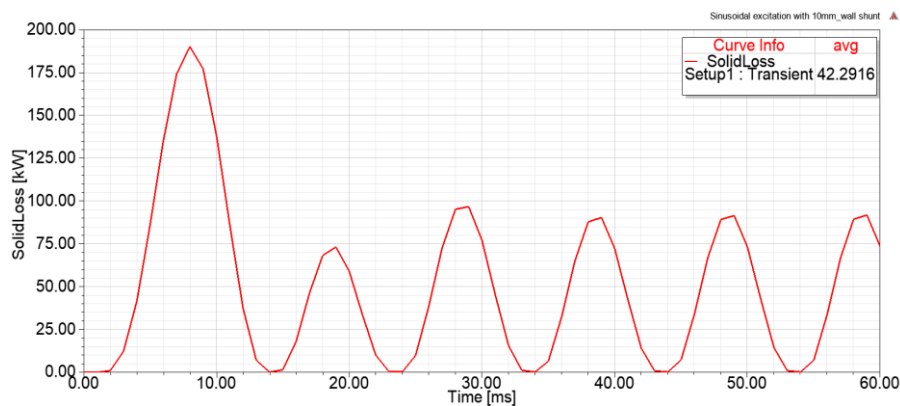


Figure 27: Waveform of Stray Loss

From Figure 25, pf of the LV winding calculated as 0.82 and efficiency is 94.69 %.

4.2.1.2 CT with 20 mm wall shunt

After simulation, induced voltage and current waveform of LV, MV and HV winding is shown in Figure 28 and Figure 29. The average value of the stray loss is 16.52 kW which is obtained from Figure 30.

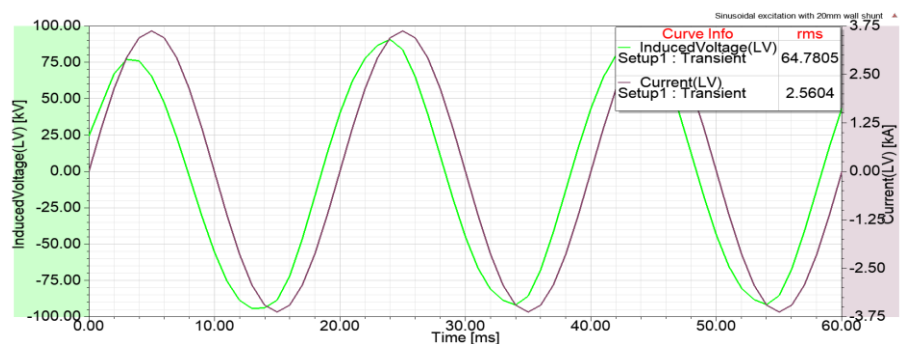


Figure 28: Waveform of LV Winding Induced Voltage and Current

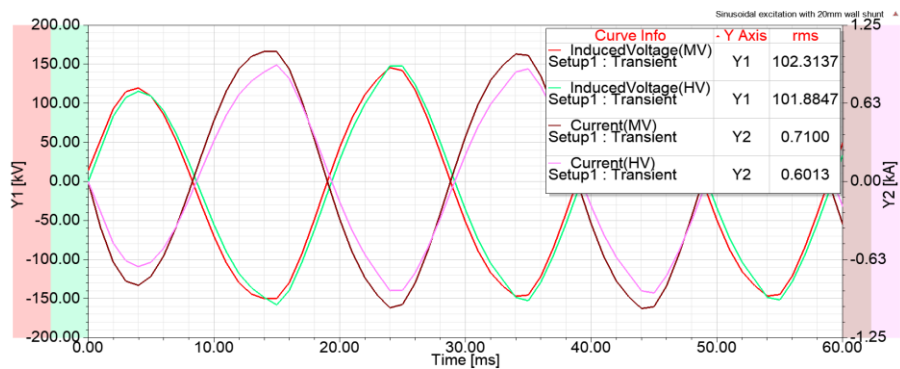


Figure 29: Induced Voltage and Current Waveforms of MV and HV Winding

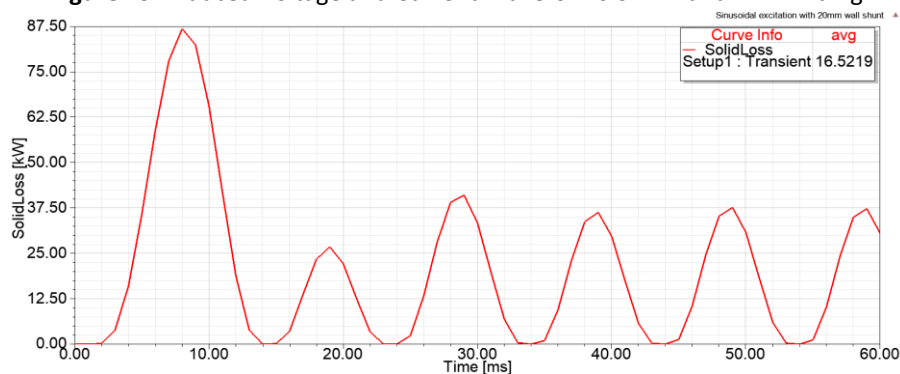


Figure 30: Waveform of Stray Loss

From **Figure 28**, pf of the LV winding calculated as 0.84 and efficiency is 96.02 %.

4.2.2. Non-Sinusoidal Current Excitation

In this section, current excitation and loading values are the same as the previous non-sinusoidal excitation with a vertical shunt.

4.2.2.1 CT with 10 mm wall shunt

After simulation, induced voltage and current waveform of LV, MV and HV winding is shown in **Figure 31** and **Figure 32**. The average value of the stray loss is 57.7 kW which is obtained from **Figure 33**.

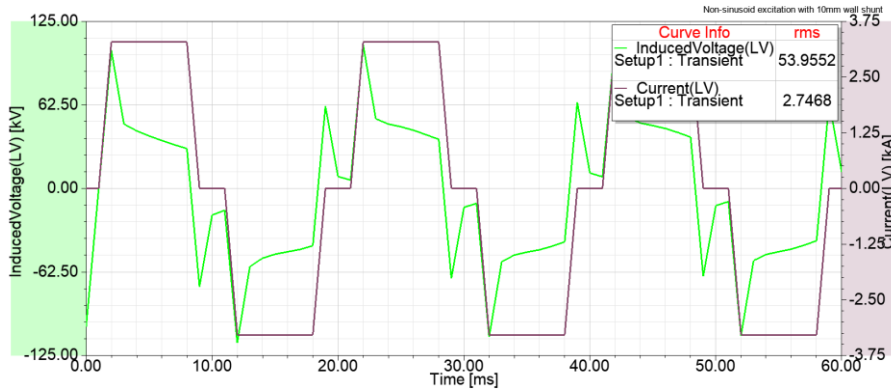


Figure 31: Waveform of LV Winding Induced Voltage and Current

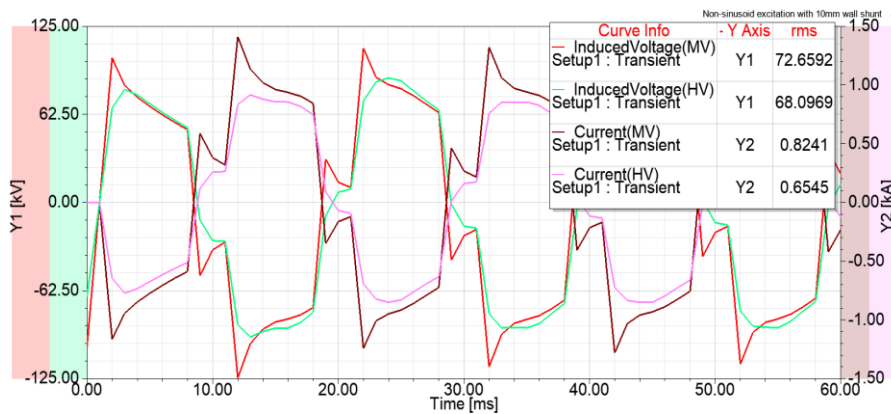


Figure 32: Induced Voltage and Current Waveforms of MV and HV Winding

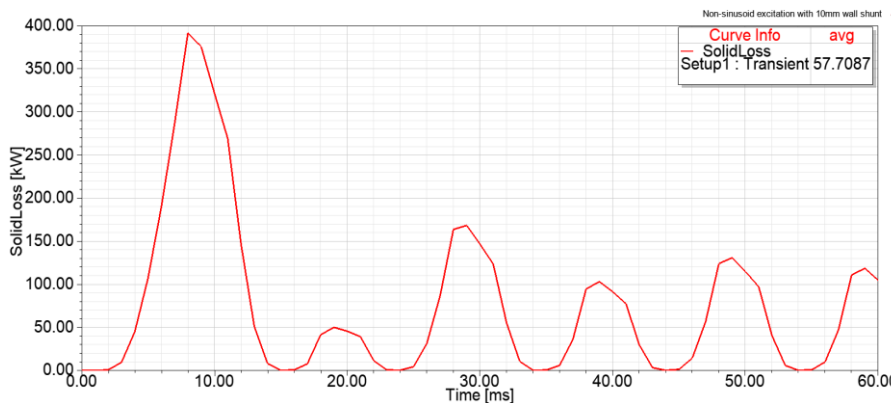


Figure 33: Waveform of Stray Loss

Using FFT analysis, the pf of the LV winding is found as 0.88 and efficiency is 80.38%.

4.2.2.2 CT with 20 mm wall shunt

After simulation, induced voltage and current waveform of LV, MV and HV winding is shown in **Figure 34** and **Figure 35**. The average value of the stray loss is 21.3 kW which is obtained from **Figure 36**.

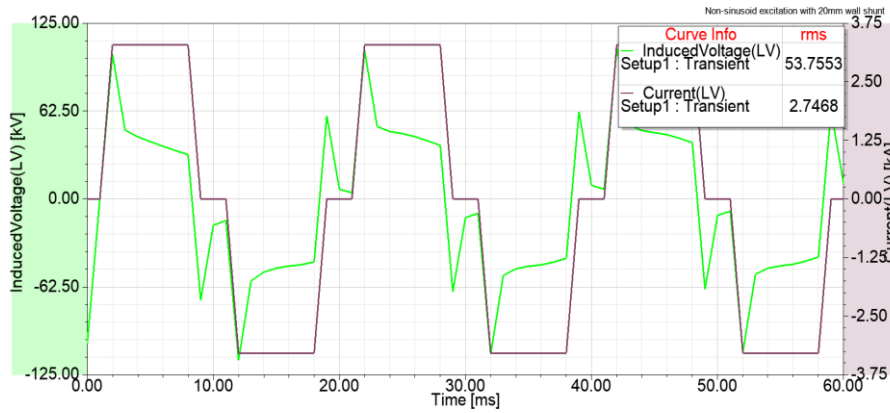


Figure 34: Waveform of LV Winding Induced Voltage and Current

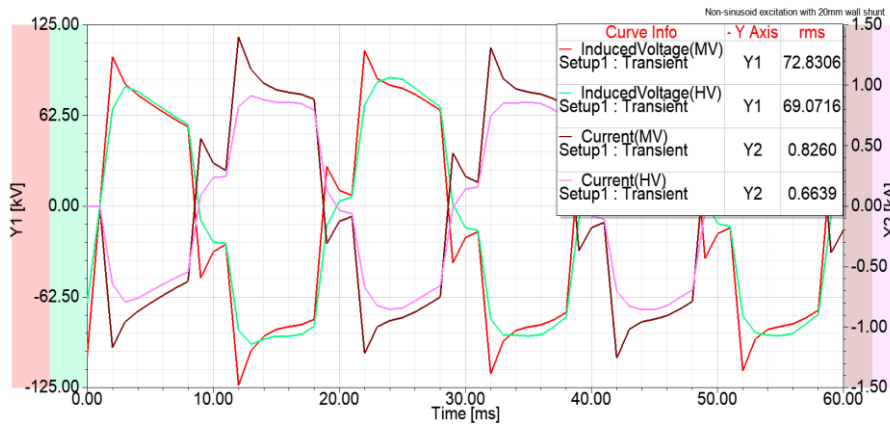


Figure 35: Induced Voltage and Current Waveforms of MV and HV Winding

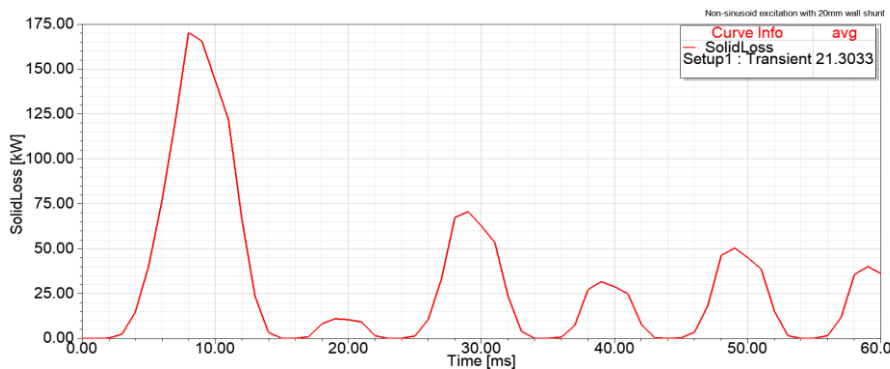


Figure 36: Waveform of Stray Loss

Using FFT analysis, the pf of the LV winding is found as 0.89 and efficiency is 81.10%.

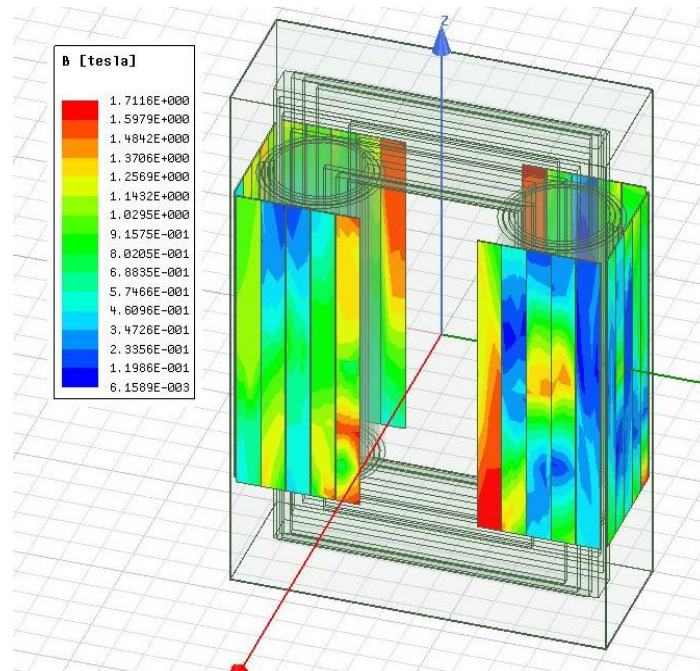


Figure 37: Magnetic Flux Density on Vertical Wall Shunt

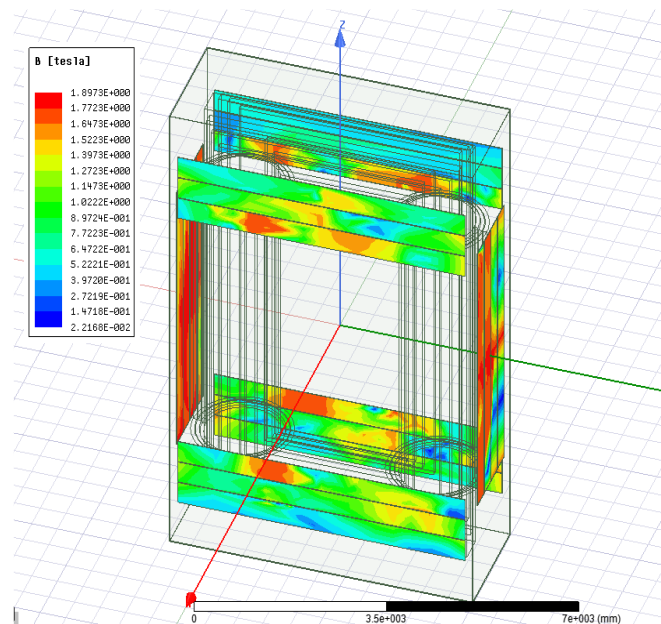


Figure 38: Magnetic Flux Density on Vertical and Horizontal Wall Shunt

Figure 37 shows that the magnetic flux density is not uniformly distributed on the vertical wall shunt and magnetic flux density at the bottom part of the vertical wall shunt is maximum. So, significantly less amount of leakage magnetic fluxes passes through this vertical wall shunt.

Figure 38 shows that magnetic flux density is uniformly distributed on the vertical and horizontal wall shunt. The maximum amount of leakage fluxes passes through this magnetic wall shunt compared with the previous vertical wall shunt case. So using FEA, magnetic wall shunt location can be optimized.

Table 3 shows that the stray loss are reduced from 114.15 kW to 18.90 kW in sinusoidal excitation and 215.4 kW to 33.74 kW in non-sinusoidal excitation; also, core losses are

reduced from 78.72 kW to 29.97 kW in sinusoidal excitation and 80.99 kW to 35.32 kW in non-sinusoidal excitation by the use of vertical wall shunt.

Sr. No.	Particulars	Sinusoidal Excitation			Non-Sinusoidal Excitation		
		Core Loss (kW)	Stray Loss (kW)	Efficiency	Core Loss (kW)	Stray Loss (kW)	Efficiency
1.	CT with tank	78.72	114.15	90.38%	80.99	215.4	78.91%
2.	CT with 10mm wall shunt	64.59	43.90	93.85%	70.42	63.52	79.68%
3.	CT with 20mm wall shunt	29.97	18.90	95.51%	35.32	33.74	80.39%

Table 3: Comparative Analysis of Vertical Wall Shunt for Both Cases

Also, from **Table 4**, it is seen that the stray loss are reduced from 114.15 kW to 16.52 kW in sinusoidal excitation and 215.4 kW to 21.30 kW in non-sinusoidal excitation; also, core losses are reduced from 78.72 kW to 24.06 kW in sinusoidal excitation and 80.99 kW to 25.35 kW in non-sinusoidal excitation by the use of horizontal wall shunt.

Sr. No.	Particulars	Sinusoidal Excitation			Non-Sinusoidal Excitation		
		Core Loss (kW)	Stray Loss (kW)	Efficiency	Core Loss (kW)	Stray Loss (kW)	Efficiency
1.	CT with tank	78.72	114.15	90.38%	80.99	215.4	78.91%
2.	CT with 10mm wall shunt	42.41	42.29	94.69%	49.92	57.70	80.38%
3.	CT with 20mm wall shunt	24.06	16.52	96.02%	25.35	21.30	81.10%

Table 4: Comparative Analysis of Horizontal Wall Shunt for Both Cases

Sr. No.	Particulars	Sinusoidal Excitation		Non-Sinusoidal Excitation	
		Analytical Method (kW)	3-D FEA Method (kW)	Analytical Method (kW)	3-D FEA Method (kW)
1.	CT with tank	110.52	114.15	222.20	215.4
2.	CT with 10mm wall shunt	43.10	43.90	63.86	63.52
3.	CT with 20mm wall shunt	19.69	18.90	32.155	33.74

Table 5: Stray Losses of Converter Transformer using Vertical Wall Shunt

In both types of wall shunt is seen that the core loss and stray loss are more in non-sinusoidal current excitation than sinusoidal current excitation as sinusoidal excitation is the fundamental component of non-sinusoidal excitation.

Sr. No.	Particulars	Sinusoidal Excitation		Non-Sinusoidal Excitation	
		Analytical Method (kW)	3-D FEA Method (kW)	Analytical Method (kW)	3-D FEA Method (kW)
1.	CT with tank	110.52	114.15	222.20	215.4
2.	CT with 10mm wall shunt	41.63	42.29	55.06	57.70
3.	CT with 20mm wall shunt	14.98	16.52	21.21	21.30

Table 6: Stray Losses of Converter Transformer using Horizontal Wall Shunt

The stray losses which are calculated by the 3-D FEA method are compared with the analytical method, as shown in **Table 5** and **Table 6** Equation (21) is used to calculate stray losses by analytical method. In equation (21), $\int_{surface} (H_a)^2 ds$ is separately calculated for each case. This integral part is evaluated by adding $(H_a)^2$ of each transformer tank's face using a field calculator of FEA software. The medium of conductivity used in the calculation is 2×10^6 mho/m, which is the conductivity of transformer tanks material.

Figure 5(a) and **Figure 5(b)** show that the total number of wall shunt used in horizontal wall shunt is less compared to vertical wall shunt. Therefore, the transformer's weight is decreased, and the transformer's cost is reduced in horizontal wall shunt compared to vertical wall shunt. Comparing **Table 3** and **Table 4** shows that the horizontal wall shunt is more effective than vertical wall shunt to reduce stray loss, core loss, and the improvement in CT efficiency. Furthermore, the increase in thickness of wall shunt stray loss is reduced.

5. CONCLUSION

In this article, CT is designed and simulated in ANSYS-MAXWELL (3D-FEA). As the CT's secondary and tertiary winding legs are connected to the rectifier, the current flowing through this transformer is non-sinusoidal, so the transformer losses are higher. Stray losses occurred in the transformer tank, which is nearly 10% to 15% of the total losses. Stray losses are reduced using the transformer tank's wall shunt, and these losses are calculated using the 3D-FEA method and verified by the analytical method. The results show that the core loss and stray loss are more in non-sinusoidal current excitation compared to sinusoidal current excitation and horizontal wall shunt is more effective than vertical wall shunt for the reduction of stray loss. As the total number of wall shunt is reduced in horizontal wall shunt, so the transformer's weight and the cost are reduced in horizontal wall shunt compared to the vertical wall shunt. Using FEA method, the location of the horizontal wall is optimized for maximum performance. Also, if wall shunt thickness increases, stray losses are reduced; hence, CT's efficiency is increased.

References

- Alassi, Abdulrahman, Santiago Bañales, Omar Ellabban, Grain Adam, and Callum MacIver. 2019. "HVDC Transmission: Technology Review, Market Trends and Future Outlook." *Renewable and Sustainable Energy Reviews* 112 (September): 530–54. <https://doi.org/10.1016/j.rser.2019.04.062>.
- Basak, A., and H. Kendall. 1987. "Leakage Flux in the Steel Tank of a 2.5-KVA Single Phase Transformer." *IEEE Transactions on Magnetics* 23 (5): 3831–35. <https://doi.org/10.1109/TMAG.1987.1065466>.
- BHEL. 2003. *Transformers*. 2nd edition. MC GRAW HILL INDIA.
- Carlson, Ake. 1996. "Specific Requirements on HVDC Converter Transformers.Pdf." *ABB Transformers* AB, 1996. <https://library.e.abb.com/public/5f6d61425208b604c1256fda004aeada/Specific%20requirements%20on%20HVDC%20converter%20transformers.pdf>.
- Carrasco, J.M., L.G. Franquelo, J.T. Bialasiewicz, E. Galvan, R.C. PortilloGuisado, M.A.M. Prats, J.I. Leon, and N. Moreno-Alfonso. 2006. "Power-Electronic Systems for the Grid Integration of Renewable Energy Sources: A Survey." *IEEE Transactions on Industrial Electronics* 53 (4): 1002–16. <https://doi.org/10.1109/TIE.2006.878356>.
- Dasgupta, Indrajit. 2009. "Power Transformers Quality Assurance". New Age International Pvt Ltd Publishers.

- Del Vecchio, Robert M., ed. 2010. "Transformer Design Principles: With Applications to Core-Form Power Transformers". 2nd ed. Boca Raton, FL: CRC Press.
- Djurovic, M., and J. Monson. 1977. "3-Dimensional Computation of the Effect of the Horizontal Magnetic Shunt on Transformer Leakage Fields." *IEEE Transactions on Magnetics* 13 (5): 1137–39. <https://doi.org/10.1109/TMAG.1977.1059658>.
- Djurovic, M., and J. E. Monson. 1982. "Stray Losses in the Step of a Transformer Yoke with a Horizontal Magnetic Shunt." *IEEE Transactions on Power Apparatus and Systems PAS-101* (8): 2995–3000. <https://doi.org/10.1109/TPAS.1982.317629>.
- Hajiaghahi, S., K. Abbaszadeh, and A. Salemnia. 2019. "A New Approach for Transformer Interturn Faults Detection Using Vibration Frequency Analysis." *Iranian Journal of Electrical and Electronic Engineering* 15 (1): 14–28. <https://doi.org/10.22068/IJEEE.15.1.14>.
- "IEEE Standard Definitions for the Measurement of Electric Power Quantities Under Sinusoidal, Nonsinusoidal, Balanced, or Unbalanced Conditions." 2010. *IEEE Std 1459-2010* (Revision of IEEE Std 1459-2000), March, 1–50. <https://doi.org/10.1109/IEEESTD.2010.5439063>.
- Jamali, M., M. Mirzaie, and S. A. Gholamian. 2011. "Discrimination of Inrush from Fault Currents in Power Transformers Based on Equivalent Instantaneous Inductance Technique Coupled with Finite Element Method." *Iranian Journal of Electrical and Electronic Engineering* 7 (3): 197–202. <http://ijeee.iust.ac.ir/article-1-342-en.html>.
- Janić, Žarko, Zvonimir Valković, and Željko Štih. 2006. "Stray Losses in Transformer Clamping Plate." In *ICEM 2006 XVII International Conference on Electrical Machines*, 1–5. Greece. <https://www.bib.irb.hr/254695?lang=en&print=true&rad=254695&table=zbornik>.
- Kimbark, Edward Wilson. 1971. "Direct Current Transmission. New York: Wiley-Interscience".
- Kothavade, Jayesh U., and Prasanta Kundu. 2021. "Investigation Of Electromagnetic Forces In Converter Transformer." In *2021 IEEE 2nd International Conference on Smart Technologies for Power, Energy and Control (STPEC)*, 1–6. <https://doi.org/10.1109/STPEC52385.2021.9718676>.
- Kuczmann, Miklós, Attila Szücs, and Gergely Kovács. 2021. "Transformer Model Identification by Ārtap: A Benchmark Problem." *Periodica Polytechnica Electrical Engineering and Computer Science* 65 (2): 123–30. <https://doi.org/10.3311/PPee.17606>.
- Kulkarni, S. V., and S. A. Khaparde. 2004. "Transformer Engineering: Design and Practice". *Power Engineering* 25. New York: Marcel Dekker, Inc.
- Li, Longnv, Wei Nong Fu, Siu Lau Ho, Shuangxia Niu, and Yan Li. 2014. "Numerical Analysis and Optimization of Lobe-Type Magnetic Shielding in a 334 MVA Single-Phase Auto-Transformer." *IEEE Transactions on Magnetics* 50 (11): 1–4. <https://doi.org/10.1109/TMAG.2014.2326465>.
- Li, Longnv, Shuangxia Niu, S. L. Ho, W. N. Fu, and Yan Li. 2015. "A Novel Approach to Investigate the Hot-Spot Temperature Rise in Power Transformers." *IEEE Transactions on Magnetics* 51 (3): 1–4. <https://doi.org/10.1109/TMAG.2014.2359956>.
- Moghaddami, Masood, Arif I. Sarwat, and Francisco de Leon. 2017. "Reduction of Stray Loss in Power Transformers Using Horizontal Magnetic Wall Shunts." *IEEE Transactions on Magnetics* 53 (2): 1–7. <https://doi.org/10.1109/TMAG.2016.2611479>.

- Oliveira, Eduardo e, Vera L. Miguéis, Luís Guimarães, and José Borges. 2017. "Power Transformer Failure Prediction: Classification in Imbalanced Time Series." *U.Porto Journal of Engineering* 3 (2): 34–48. https://doi.org/10.24840/2183-6493_003.002_0004.
- "Optimal Placement of a Wall-Tank Magnetic Shunt in a Transformer Using FE Models and a Stochastic-Deterministic Approach | IEEE Conference Publication | IEEE Xplore." n.d. Accessed March 8, 2023. <https://ieeexplore.ieee.org/document/1633258>.
- Orosz, Tamás, Bence Borbély, and Zoltán Ádám Tamus. 2017. "Performance Comparison of Multi Design Method and Meta-Heuristic Methods for Optimal Preliminary Design of Core-Form Power Transformers." *Periodica Polytechnica Electrical Engineering and Computer Science* 61 (1): 69–76. <https://doi.org/10.3311/PPee.10207>.
- Orosz, Tamás, Péter Sörös, Dávid Raisz, and Ádám Z. Tamus. 2015. "Analysis of the Green Power Transition on Optimal Power Transformer Designs." *Periodica Polytechnica Electrical Engineering and Computer Science* 59 (3): 125–31. <https://doi.org/10.3311/PPee.8583>.
- Park, Keun-Ho, Hak-Ju Lee, and Sung-Chin Hahn. 2019. "Finite-Element Modeling and Experimental Verification of Stray-Loss Reduction in Power Transformer Tank With Wall Shunt." *IEEE Transactions on Magnetics* 55 (12): 1–4. <https://doi.org/10.1109/TMAG.2019.2940825>.
- Poblador, Martha L. Angarita, and Gustavo A. Ramos López. 2013. "Power Calculations in Nonlinear and Unbalanced Conditions According to IEEE Std 1459-2010." In *2013 Workshop on Power Electronics and Power Quality Applications (PEPQA)*, 1–7. <https://doi.org/10.1109/PEPQA.2013.6614957>.
- Sadiku, Matthew N. O. 2015. "Elements of Electromagnetics". Sixth edition. The Oxford Series in Electrical and Computer Engineering. New York: Oxford University Press.
- Sawhney, A. K., Shiv Singh Meena, and B. Tech. 2014. "Electrical Machine Design". 6th ed. Vol. 6. Delhi: Dhanpat Rai. <https://www.worldcat.org/pt/title/802763397>.
- Song, Zhanhai, Yifang Wang, Shuai Mou, Zhe Wu, Yinhui Zhu, Bingfu Xiang, and Ce Zhou. 2011. "Tank Losses and Magnetic Shunts in a Three Phase Power Transformer." In , 1–4. Greece. <https://doi.org/10.1109/ICEMS.2011.6074005>.
- Susnjic, Livio, Zijad Haznadar, and Zvonimir Valkovic. 2008. "3D Finite-Element Determination of Stray Losses in Power Transformer." *Electric Power Systems Research* 78 (10): 1814–18. <https://doi.org/10.1016/j.epsr.2008.03.009>.
- Thango, Bonginkosi A., and Pitshou N. Bokoro. 2022. "Stray Load Loss Valuation in Electrical Transformers: A Review." *Energies* 15 (7): 2333. <https://doi.org/10.3390/en15072333>.
- Thango, Bonginkosi A., Jacobus A. Jordaan, and Agha F. Nnachi. 2021. "Analysis of Stray Losses in Transformers Using Finite Element Method Modelling." In *2021 IEEE PES/IAS PowerAfrica*, 1–5. <https://doi.org/10.1109/PowerAfrica52236.2021.9543100>.
- Wang, Xuan, Juanjuan Yang, Xiaolong Cao, Man Xu, and Jingshun Lv. 2003. "The Electric Tests of Ordinate Insulation in Converter Transformer by the Method of Applying Voltage on Single-Phase." In *Proceedings of the 7th International Conference on Properties and Applications of Dielectric Materials (Cat. No.03CH37417)*, 3:1170–73 vol.3. <https://doi.org/10.1109/ICPADM.2003.1218632>.